TISSUE ENGINEERING: Part C
Volume 19, Number 5, 2013

DOI: 10.1089/ten.tec.2012.0423

Influence of Cyclic Mechanical Stretch and Tissue Constraints on Cellular and Collagen Alignment in Fibroblast-Derived Cell Sheets

Nathan K. Weidenhamer, BS,[1] and Robert T. Tranquillo, PhD[1,2]

Mechanical forces play an important role in shaping the organization of the extracellular matrix (ECM) in developing and mature tissues. The resulting organization gives the tissue its unique functional properties. Understanding how mechanical forces influence the alignment of the ECM is important in tissue engineering, where recapitulating the alignment of the native tissue is essential for appropriate mechanical anisotropy. In this work, a novel method was developed to create and stretch tubular cell sheets by seeding neonatal dermal fibroblasts onto a rotating silicone tube. We show the fibroblasts proliferated to create a confluent monolayer around the tube and a collagenous, isotropic tubular tissue over 4 weeks of static culture. These silicone tubes with overlying tubular tissue constructs were mounted into a cyclic distension bioreactor and subjected to cyclic circumferential stretch at 5% strain, 0.5 Hz for 3 weeks. We found that the tissue subjected to cyclic stretch compacted axially over the silicone tube in comparison to static controls, leading to a circumferentially aligned tissue with higher membrane stiffness and maximum tension. In a subsequent study, the tissue constructs were constrained against axial compaction during cyclic stretching. The resulting alignment of fibroblasts and collagen was perpendicular (axial) to the stretch direction (circumferential). When the cells were devitalized with sodium azide before stretching, similarly constrained tissue did not develop strong axial alignment. This work suggests that both mechanical stretching and mechanical constraints are important in determining tissue organization, and that this organization is dependent on an intact cytoskeleton.

Introduction

The development of cell-derived tissue from extended culture of plated cells, also known as a "cell sheet," is a popular tissue engineering strategy. Utilizing this approach, mesenchymal cells such as fibroblasts,[1–3] smooth muscle cells,[2,4,5] and mesenchymal stem cells[5,6] have been cultured and stimulated to secrete a collagenous extracellular matrix (ECM). After several weeks of culture, the resulting tissue sheet of nominal thickness 20 μm can be removed from the substrate by mechanical peeling or with a temperature change[7] and layered to form thicker, mechanically robust tissues. Cell sheet technology has been widely used in the development of engineered tissues such as blood vessels, myocardium, cornea, esophagus, and trachea.[8]

Since both the cells and ECM of cardiovascular tissues exhibit a characteristic alignment,[9] there is a need to develop techniques to generate alignment in cell sheets in order to confer the correct biological and mechanical properties. Techniques such as micropatterning have been widely used to control cell behavior, influence tissue alignment, and dictate mechanical properties. Williams *et al.* found that 20-μm-wide by 5-μm-deep grooves on a fibronectin-coated PDMS substrate provided the appropriate environment to allow human mesenchymal stem cells to align with the grooves. Furthermore, tissues that were between 10–15 μm thick also showed alignment with the pattern direction.[4] Similarly, bovine aortic smooth muscle cells cultured on micropatterned substrates showed alignment in the pattern direction, as well as a higher failure stress and stiffness in the pattern direction, indicating mechanical anisotropy.[4] However, other studies show that the alignment of the tissue is only maintained in tissues under 20 μm thick, after which the cell layers could not sense the contact guidance cues presented by the patterned substrate leading to an isotropic microstructure. This result suggests a limit to the number of cell layers that can sense the underlying substrate pattern.[10]

Mechanical strain has also been explored as a means to create alignment in cell sheets. Both static mechanical strain and cyclic mechanical strain have been considered. In one study, fibroblast cell sheets were physically constrained on two edges but allowed to freely compact inward along the

Departments of [1]Biomedical Engineering and [2]Chemical Engineering & Materials Science, University of Minnesota, Minneapolis, Minnesota.

other two edges for 21 days.[11] Over the course of the experiment, the cells and ECM aligned parallel to the constrained direction and showed a higher failure stress and stiffness in the aligned direction. Another study compared the difference between static stretch (as above) and cyclic stretch (10% stretch, 1 Hz) on the alignment and mechanical properties of similarly constrained fibroblast cell sheets.[12] This study found that both static stretch and cyclic stretch led to an alignment of the fibroblasts in the stretch direction, but that cyclic stretch improved mechanical anisotropy relative to static stretch. One difficulty in interpreting these studies comes from the fact that the cell sheets were permitted to compact in the direction that was not mechanically stretched. This makes it difficult to determine whether the source of alignment is due to the cells and ECM reorganizing in response to local mechanical strain, stress, and related effects, or if alignment is due to macroscopic compaction of the tissue and resultant reorientation of the cells and ECM.

In this study, we hypothesized that there is an interaction between cyclic mechanical stretch and the mechanical constraints placed on the tissue (i.e., preventing or allowing compaction) that ultimately determines the alignment of the cells and ECM. Since cell sheets that are grown and stretched on a planar substrate peel off within a week (unpublished data), we decided to form the tissue around a distensible silicone tube since a tubular tissue cannot peel away from its substrate, permitting long-term stretching. In order to investigate the hypothesis, we developed three goals: (1) to develop a technique to seed fibroblasts uniformly onto a tubular substrate, (2) to modify our existing cyclic distention bioreactor[13,14] to accommodate silicone tubing on which a cell sheet is growing, and (3) to determine the influence of long-term cyclic stretch and mechanical constraints on cellular and ECM alignment.

Materials and Methods

Cell culture

Neonatal human dermal fibroblast (nHDF; Clonetics) were maintained in a 50/50 mixture of Dulbecco's modified Eagle's medium and Ham's F12 cell culture medium (DMEM/F12; Cellgro) supplemented with 15% fetal bovine serum (FBS; Thermo-Fisher Scientific), 100 U/mL penicillin, and 100 μg/mL streptomycin. Cells were incubated at 37°C in 100% humidity and 5% CO2, passaged at ~90% confluency, and harvested for use at passage 9.

Cell seeding and static culture

nHDF were seeded directly onto a segment of 2-mm outer-diameter silicone tubing (Vesta, Inc.) that was weighted with a PTFE-coated segment of stainless steel wire (McMaster-Carr) placed through the lumen. The silicone tubing was passively coated with 25 μg/mL of bovine fibronectin (Sigma) for 1 h before cell seeding. The tubing was placed inside a vented 50 cc conical tube (TPP) with 5 mL of nHDF suspension in DMEM/F12 (3:1) with 10% FBS, 100 U/mL penicillin, and 100 μg/mL streptomycin. The 50 cc conical tube was placed horizontally into a CELLROLL System (Integra Biosciences AG) and set to roll at 2 rpm overnight (Fig. 1A). After the rolling period, the cell-seeded tubing was placed into six-well plates with a custom-made Teflon insert and maintained in DMEM/F12 (3:1) with 10% FBS, 100 U/mL penicillin, 100 μg/mL streptomycin, 50 μg/mL ascorbic acid (Sigma), 2 μg/mL insulin (Sigma), and 5 μg/mL epidermal growth factor (EGF; Calbiochem) for 4 weeks. Complete medium changes occurred three times weekly.

Bioreactor culture

Cell-seeded silicone tubing was mounted into a customized cyclic distension bioreactor previously described,[13] by first sliding the tubing off of the PTFE-coated stainless steel wire. In experiments where the tissue was constrained axially, a 2–0 silk suture (Fine Science Instruments) was tied at the ends of the tissue before sliding the tubing off of the wire. Once removed from the wire, the ends of the tubing were tied to the barbed ends of a 1/8" male luer connector (Value Plastics, Inc.). One end of the luer connector was plugged with a female luer cap and the other end was connected to a pressurized airline (Fig. 1B). The whole system was placed in a jar containing 60 mL of DMEM/F12 (3:1) with 10% FBS, 100 U/mL penicillin, 100 μg/mL streptomycin, 250 ng/mL Amphotericin B (Cellgro), 50 μg/mL ascorbic acid, 2 μg/mL insulin, and 5 μg/mL EGF for 3 weeks, with 70% of the medium changed three times weekly. Cyclically stretched samples were stretched as follows: the frequency and duty of the air cycle were controlled by a solenoid valve connected downstream of a pressure regulator. A laser micrometer was used to measure the diameter of the tube at different inlet air pressures, and a pressure–diameter correlation was recorded (Fig. 1C), which was used to set the maximum strain for each experiment. The maximum circumferential strain (stretch) magnitude that could be applied reliably was 5%. For all studies, a 5% stretch magnitude and a stretch frequency of 0.5 Hz with 12.5% duty cycle, corresponding to a 0.25 s stretch time in a 2 s cycle period, were used. Static controls were mounted into bioreactors and not subjected to cyclic pressurization/stretch.

Azide treatment

In order to determine the contribution of cells to any stretch-induced alignment, samples were devitalized by treatment with sodium azide. Four-week-old cell-seeded tubing was treated with 0.5% sodium azide (Sigma), 10 mM EDTA (Sigma), 1 μg/mL Pepstatin A (Sigma), and 1 μg/mL Aprotinin (Sigma) for 1 week after being mounted in the bioreactor with sutures for axial constraint, but before stretching was initiated. After the azide treatment period, the tissue was maintained in DMEM with 10% FBS, 100 U/mL penicillin, and 100 μg/mL streptomycin until harvest after 3 weeks of stretching. Cyclic stretch experiments were conducted as described above.

Polarized light imaging

Polarized light imaging was conducted as previously described.[15] Briefly, a fiber source (Technispec), focusing lens (Edmund Scientific), and computer-controlled rotation (Mill-Shaf Technologies) of a linear polarizer sheet (Edmund Scientific) provided wide-field illumination of a sample with linearly polarized light of variable transmission axes. Images were acquired in transmission mode at each of 20 rotation angles of the linear polarizer over the range of 0–180 degrees

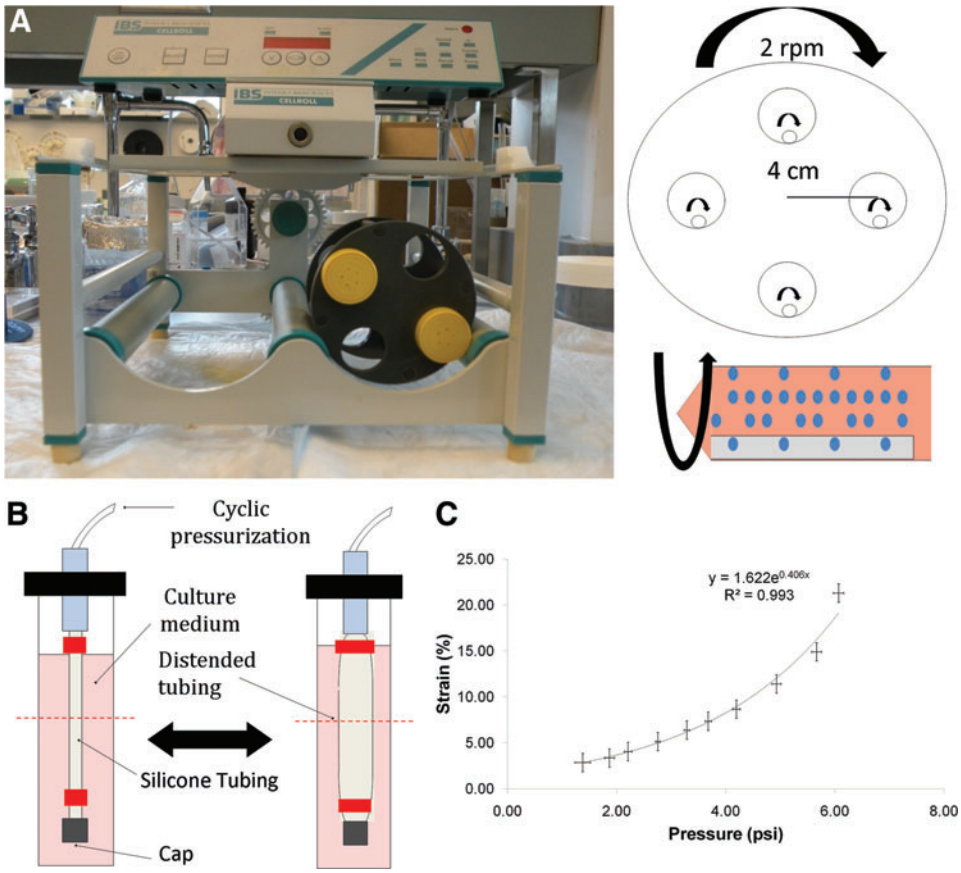

FIG. 1. **(A)** Front view and schematic of the CellRoll system used to seed fibroblasts onto silicone tubing. 50 mL conical tubes were placed within the tubing rack and rolled at 2 rpm. The silicone tubing rolled within the 50 mL conical, allowing cells to settle onto the entire area of the tubing. **(B)** Diagram of the cyclic distension bioreactor used in this study. Silicone tubing is mounted, capped on one end, and subjected to cyclic air pressurization. Red segments indicate where constraints were applied and the dashed red line indicates the plane of histological sectioning. **(C)** Circumferential strain versus pressure relation for the silicone tubing used in this study. Color images available online at www.liebertpub.com/tec

with a CCD device camera (Hitachi) and an effective circular analyzer made from a linear polarizer and a quarter-wave sheet (Oriel). Acquisition and image processing were done in Labview (National Instrument) and Matlab (MathWorks), respectively.

Uniaxial mechanical testing

Rings of tissue cut from each sample were tested for tensile properties. The dimensions of the sample were measured using calipers. The thickness of each sample was measured using a 50 *g* force probe attached to a displacement transducer. Tissue rings were placed over two T-style grips, attached to the actuator arms and load cell of an Instron MicroBionix (Instron Systems) and straightened with an applied load of 0.005 N. This position was used as the reference length of the ring. Following six cycles of 0%–10% strain conditioning at 2 mm/min, rings were stretched to failure at the same rate. True strain was calculated based on the natural log of length of the tissue over time divided by the initial length. The stress was calculated as force divided by the initial cross-sectional area. The tangent modulus (E) was determined as the slope of the linear region of the stress-strain curve before failure. The peak stress was defined as ultimate tensile strength (UTS). Membrane stiffness and maximum tension were defined as E and UTS multiplied by thickness, respectively.

Collagen and cell quantification

Collagen content was quantified using a hydroxyproline assay previously described, assuming 7.46 mg of collagen per 1 mg of hydroxyproline.[16] The sample volume was calculated using the measured length, width, and thickness of the strips (as described above in uniaxial mechanical testing). The cell content was quantified with a modified Hoechst assay for DNA assuming 7.7 pg of DNA per cell.[17] Cell concentrations were calculated as the number of cells per unit volume using the measured dimensions of the strip. Live/Dead staining (Invitrogen) was conducted per the manufacturer's recommendations.

Histology

Samples that were removed from the tubing were fixed for 1 h in 4% paraformaldehyde, infiltrated with a solution of 30% sucrose and 5% DMSO, frozen in OCT (Tissue-Tek), and sectioned into 9 μm cross sections. Samples that remained adherent to the tubing were embedded in paraffin and sectioned into 9 μm cross sections. Sections were stained with hematoxylin and eosin (H&E), Lillie's Trichrome, and picrosirius red. Images were taken with a color CCD camera. For picrosirius red, images were taken with the samples placed between crossed polarizers.

Immunostaining of tissue sections

Samples were left on the silicone tubing and fixed for 1 h in 4% paraformaldehyde. Samples were cut into segments for histological staining, rinsed with PBS, and blocked in 5% normal donkey serum for 1 h. Samples were incubated in 5 μg/mL rabbit anti-human collagen I (Novus) overnight at 4°C, and rinsed in PBS. Samples were then incubated in 4 μg/mL donkey anti-rabbit Cy3 (Jackson) overnight at 4°C.

Samples were then permeabilized with 0.1% Triton-X for 1 h, rinsed in PBS, and incubated in 15 μg/mL Oregon Green-conjugated phalloidin (Invitrogen) overnight at 4°C. Samples were visualized with a Zeiss LSM 510 Meta Confocal microscope by taking z-stacks at a spacing of 3–5 μm. The image was "flattened" by taking the maximum projection of the z-stack. Each 500×500 μm image represents ~1% of the sample.

Two-dimensional fast Fourier transform

Alignment of F-actin and collagen was determined using a two-dimensional (2D) fast Fourier transform (FFT) method.[18] Briefly, a max-projection of the image was imported to ImageJ (NIH). The image was converted to 8-bit grayscale format, and the 2D FFT function was used to generate a FFT image. 2D FFT spectra displayed varying intensities that represented the magnitude of different frequencies in the images. Isotropic images had circular spectra of bright pixels; anisotropic images had elliptical 2D FFT spectra shifted 90° from the input image's preferred angle of orientation. This 90° shift is because the 2D FFT revealed rapid changes in pixel intensity, which occurred at high frequency perpendicular to the direction of cell or fiber alignment, while along the direction of cell or fiber alignment, little change was detected and the frequency was thus low. The oval-profile plugin (http://rsbweb.nih.gov/ij/plugins/oval-profile.html) was used to determine the intensity of the FFT as a function of angle over 180°, with discrete sampling every 1°. Intensity data was normalized to the minimum intensity and the peak angle was determined as the angle at which the intensity was maximum.

Statistics

For all experiments, $n=3$ or higher sample number was used, unless otherwise indicated. See Appendix Figure A1 for a complete table of the number of samples analyzed for each experiment. Statistical significance of differences between groups was determined using Student's *t*-test for two treatments and one-way ANOVA for more than two treatments with the Fisher's Least Significant Difference (LSD) *post hoc* test in GraphPad Prism® software for Windows. Kolmogorov-Smirnov tests were conducted in MATLAB. Error bars in plots represent the standard error of the mean. Any reference to a difference in the Results and Discussion sections implies statistical significance at the level $p<0.05$, unless otherwise indicated.

Results

Cell seeding experiments

The optimal seeding conditions were found by varying cell seeding density and the time spent in the CellRoll system. At harvest, the silicone tubing was cut into five segments of equal size and the number of adhered cells was quantified. A seeding density of 1.0 M/mL yielded more adhered cells than a 0.4 M/mL seeding density, but was not statistically different than a 2.0 M/mL seeding density (Fig. 2A). There was no statistical difference in the number of adhered cells between a 4 h incubation time and an overnight incubation time (Fig. 2B). Therefore, all further experiments were conducted with a 1.0 M/mL cell seeding density and were maintained in the CellRoll system overnight.

A macroscopic view of the cell-seeded silicone tubing is shown in Figure 2C. The cell distribution and viability along the length of the silicone tubing was determined by Live/Dead staining. The cells were nearly all viable, with only a few dead cells found per field. While the cell distribution along the length was initially nonuniform, a confluent monolayer of cells developed after 1 week (Fig. 2D, E).

Cyclic stretch–unconstrained tissue

After 4 weeks of static culture, samples were mounted into the cyclic distension bioreactor, without any axial constraint on the tissue. One group of samples was cyclically stretched at 5% circumferential strain at a frequency of 0.5 Hz. The control group was mounted in the bioreactor, but was not stretched. After 3 weeks of stretching, the samples were harvested for analysis.

Macroscopic appearance. Stretched samples compacted extensively to a final length of 2.6±0.5 mm from an initial length of 20 mm, whereas the static samples compacted to a final length of 9.1±2.1 mm. The stretched samples were also

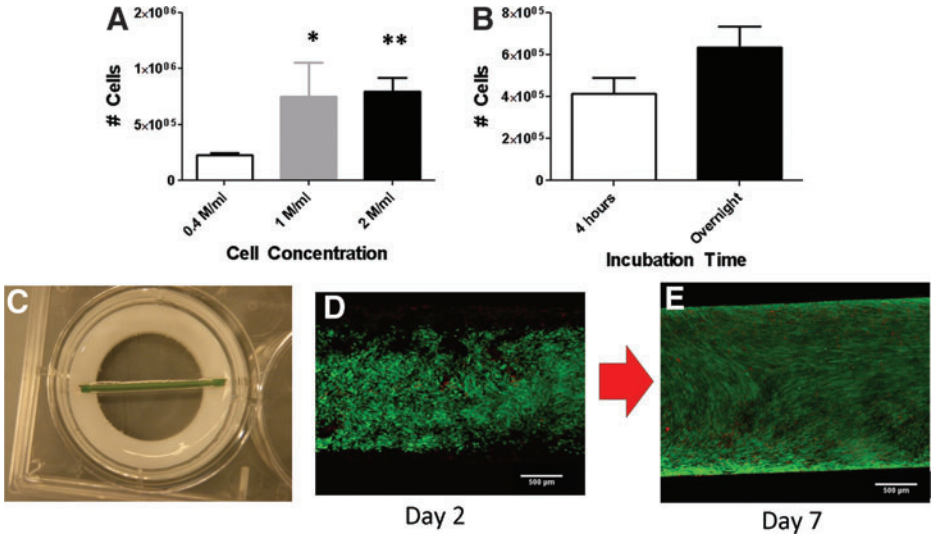

FIG. 2. Influence of **(A)** seeding density and **(B)** incubation time on the number of cells adhered to the silicone tubing. With the exception of **(A)**, all incubation times were overnight. **(C)** Macroscopic view of cell-seeded silicone tubing. Live/Dead staining of silicone tubing **(D)** immediately after seeding and **(E)** 1 week after seeding. * indicates $p<0.05$ compared to 0.4 M/ml, ** indicates $p<0.01$ compared to 0.4 M/ml. Scale bar = 500 μm. Color images available online at www.liebertpub.com/tec

thicker (160 ± 12 μm) than the static samples (79 ± 6 μm). When analyzed under polarized light, the stretched samples were highly aligned in the circumferential direction, as indicated by the red segments of the polarimetric alignment image in Figure 3A. Red dashed lines in Figure 3A indicate the boundary of the tissue, with the remainder of the area being composed of the silicone tubing. Note that there was no detectable alignment in areas with silicone tubing alone. In comparison, the static samples showed no detectable alignment (Fig. 3B).

Histology. H&E staining of sections show that cells were uniformly dispersed throughout the tissue in both the stretched and static samples, with the stretched samples being thicker (Fig. 4A, D) as noted above. Lillie's Trichrome staining revealed the tissue was primarily composed of collagen that was distributed uniformly throughout the tissue (Fig. 4B, E). Larger collagen fibrils appeared birefrigent under polarized light after staining with picrosirius red. (Fig. 4C, F).

Mechanical and biochemical properties. Stretched samples had a higher circumferential membrane stiffness (1068 ± 222 N/m vs. 399 ± 58 N/m) and maximum tension (101.4 ± 21.3 N/m vs. 42.4 ± 7.8 N/m) than static samples (Fig. 5A, B). However, the intrinsic properties, the modulus (6.7 ± 1.5 MPa stretch, 5.0 ± 1.0 MPa static) and UTS (642 ± 141 kPa stretch vs. 537 ± 83 kPa static), did not show statistical differences between stretched and static samples (Fig. 5C, D). These results indicate that the collagen network in cyclically stretched tissue was maintained as it compacted, but cyclic stretch at the 5% strain used did not improve intrinsic mechanical properties.

There was no statistical difference in cellularity between stretched and static samples (210 ± 73 M/mL stretch vs. 270 ± 60 M/mL static) (Fig. 5E). The collagen content as a percentage of total protein was lower in static samples [10.0% ± 0.2% stretch vs. 13.0% ± 0.3% static (Fig. 5F)]. However, there was no difference in collagen concentration (Fig. 5G) nor in the collagen produced per cell (Fig. 5H) between the stretched and static samples, indicating that there was no intrinsic difference in a cell's ability to produce collagen.

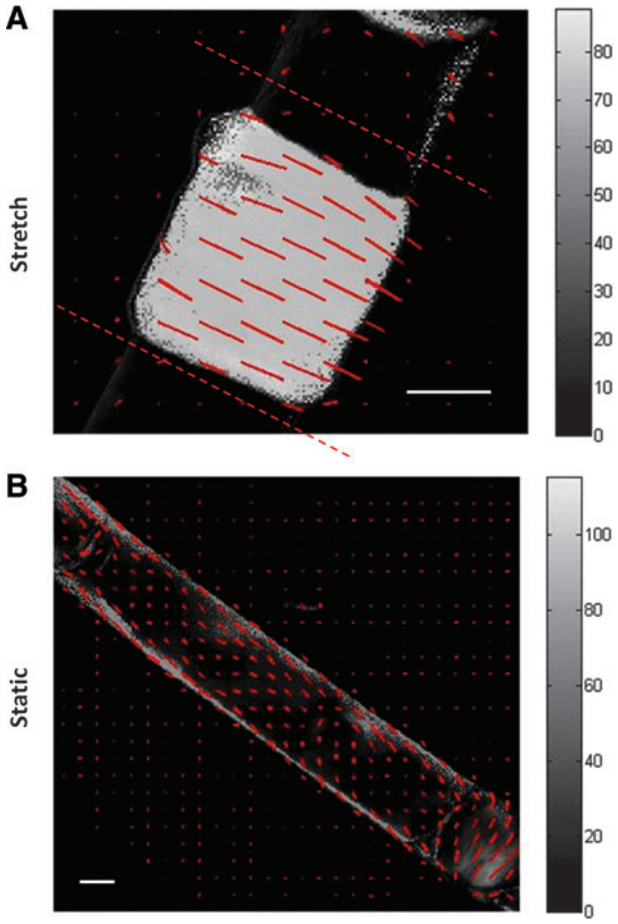

FIG. 3. Polarized light image of **(A)** stretched and **(B)** static tissue after 3 weeks of bioreactor culture. Red segments indicate the local average direction and strength of alignment (retardation), with the gray level mapped to the retardation at each pixel. Dashed lines indicate the edge of the tissue. Scale bar = 1 mm. Color images available online at www.liebertpub.com/tec

Cyclic stretch–constrained tissue

After 4 weeks of static culture, samples were mounted into the cyclic stretch bioreactor, and the tissue was constrained from compacting axially (shortening) by tying a suture onto each end. After 3 weeks of stretching at 5% circumferential strain at a frequency of 0.5 Hz, the samples were harvested for analysis.

In studies where the tissue was devitalized with sodium azide treatment, tissues were mounted in the bioreactor in a sodium azide solution for 1 week prior to the start of stretching. One group of samples was then stretched at 5% circumferential strain at a frequency of 0.5 Hz. The control group was also mounted in the bioreactor and treated with the sodium azide solution for 1 week, but was not stretched.

Histology. H&E staining of sections show that cells were uniformly dispersed throughout the tissue in both the stretched and static samples (Fig. 6A, C). Unlike the unconstrained tissue, axial constraints prevented the tissue from shortening, and the resulting thicknesses were similar. Lillie's Trichrome staining again revealed that the tissue was primarily composed of collagen distributed uniformly throughout the tissue (Fig. 6B, D). There were no obvious differences in picrosirius red staining (data not shown).

Cellular and ECM alignment. Stretched and static samples were immunostained for Type I Collagen and F-actin, and the alignment directions for each were determined by 2D FFT. When static tissue was prevented from shortening via axial constraint, samples displayed alignment, but when multiple samples were analyzed, there appeared to be no preferred alignment direction (Fig. 7A, C, G). This is in contrast to samples that were never mounted in the bioreactor (premount), which showed different local alignment directions within the same sample. However, when the tissue was axially constrained and stretched, only axial alignment was observed (Fig. 7B, D, G). The Kolmogorov-Smirnov test demonstrated that the sampling of angles in stretched tissue is statistically different from a uniform distribution ($p = 0.0018$). The results demonstrate that axial compaction is necessary to allow for circumferential cell and collagen alignment at this magnitude of cyclic stretch.

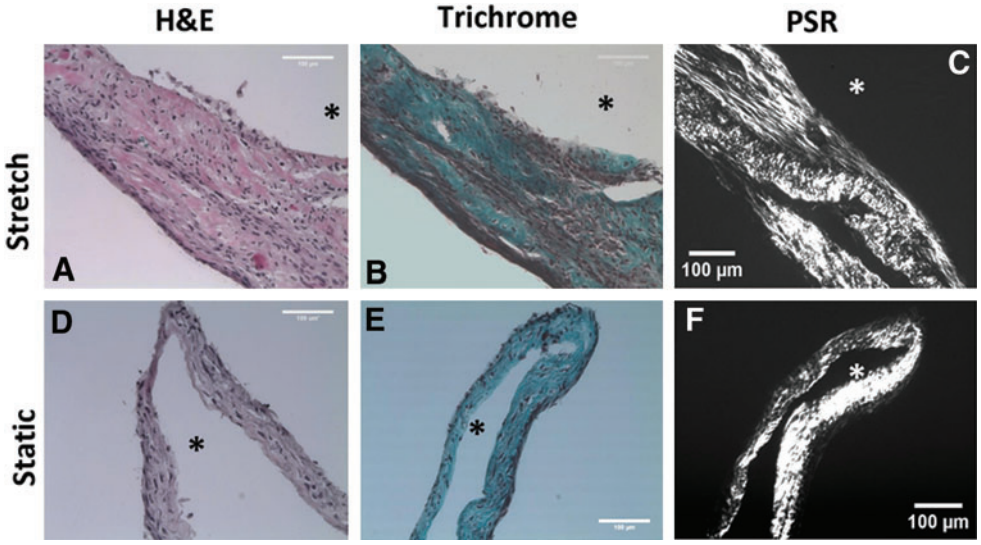

FIG. 4. Hematoxylin & eosin (H&E), Lillie's Trichrome, and picrosirius red stained sections of unconstrained tissue, stretched **(A–C)** and static **(D–F)**. Scale bar = 100 μm. * indicates position of the lumen of the tubular cell sheet. Color images available online at www.liebertpub.com/tec

Next, the tissue was devitalized with a sodium azide treatment just prior to cyclic stretching, in order to determine the role of cytoskeletal tension in the development of the observed axial alignment of collagen with cyclic stretching. Figure 7E and F show representative collagen staining in azide-treated static and stretched tissue, respectively. Note that the F-actin staining in Figure 7E and F is punctate, indicating cytoskeletal disorganization. In contrast to results for the untreated tissue presented above, the Kolmogorov-Smirnov test demonstrated that the sampling of angles in

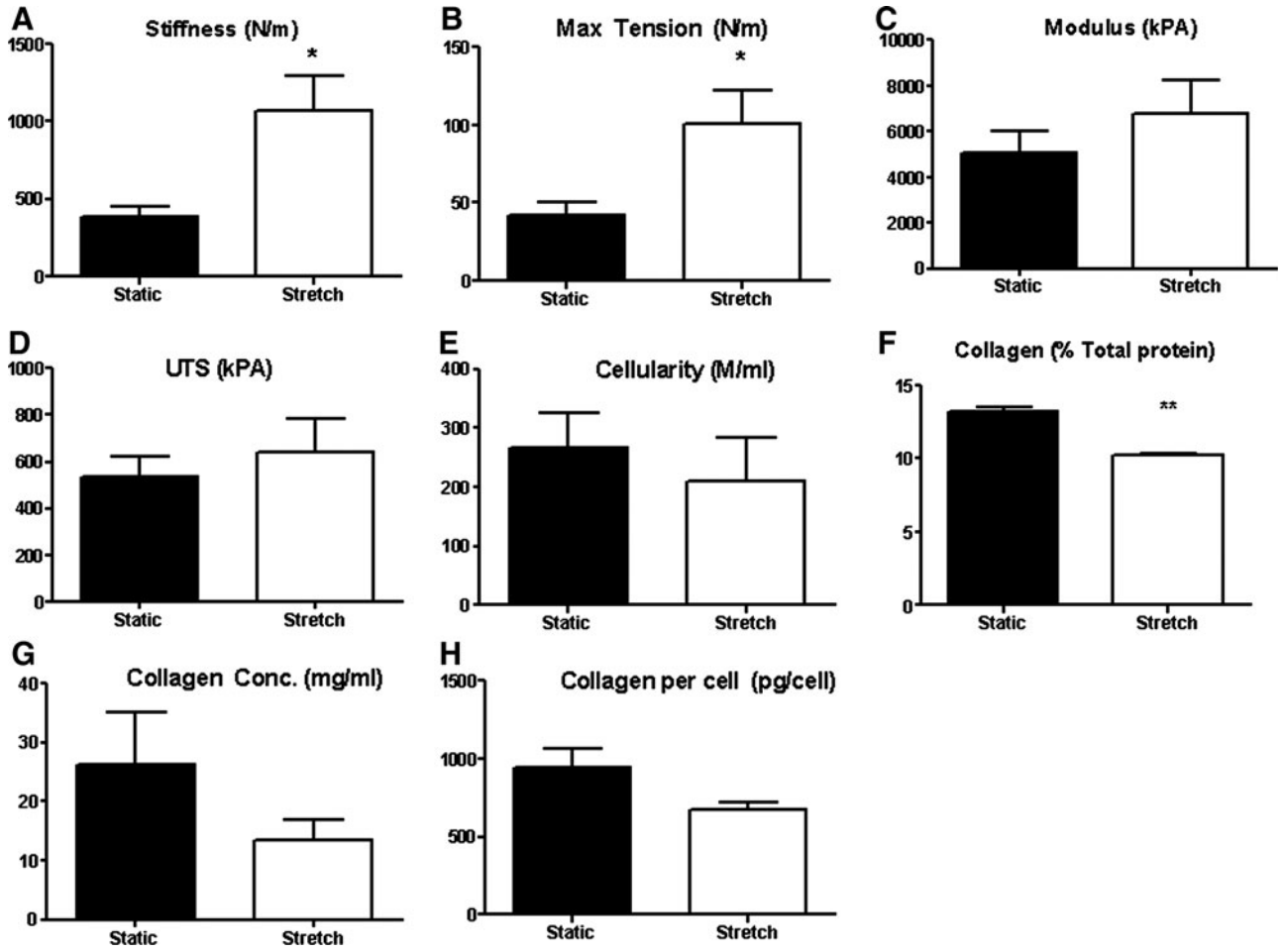

FIG. 5. Plots of physical properties of unconstrained tissue: **(A)** stiffness, **(B)** maximum tension, **(C)** modulus, **(D)** Ultimate tensile strength (UTS). Plots of biochemical properties of unconstrained tissue: **(E)** cellularity, **(F)** collagen (% total protein), **(G)** collagen concentration (mg/mL), and **(H)** collagen per cell * indicates $p < 0.05$, ** indicates $p < 0.01$.

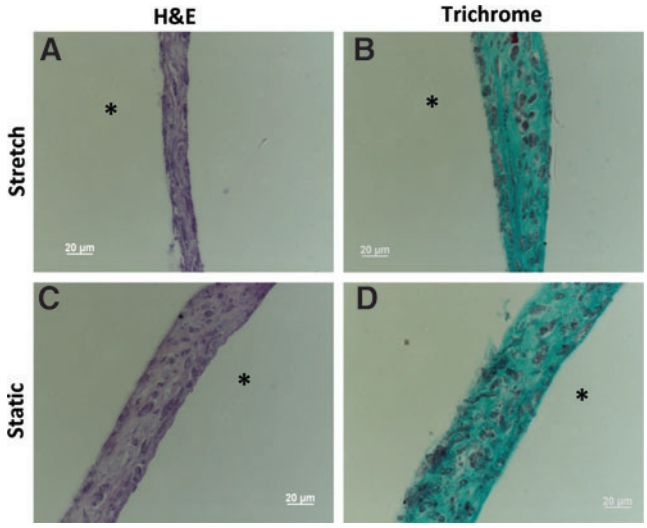

FIG. 6. H&E and Lillie's Trichrome stained sections of constrained tissue, stretched **(A, B)** and static **(C, D)**. Scale bar = 20 μm. * indicates position of the lumen of the tubular cell sheet. Color images available online at www.liebertpub.com/tec

stretched tissue that was azide treated was statistically indistinguishable from a uniform distribution ($p = 0.08$, Fig. 7F). Notwithstanding, the mean angles for stretched tissue and static controls were different, for reasons that are unclear.

Discussion

In this work, a novel seeding method that allows for direct seeding of viable cells onto the outer surface of a distensible silicone tube was developed. While similar techniques have been used to seed porous biomaterials with high efficiency,[19,20] to our knowledge this is the first study demonstrating successful cell seeding onto the outer surface of a nonporous surface. Although the seeding efficiency is low (~15%), the nHDF proliferated to form a confluent monolayer around the tube within 1 week and a robust, collagenous tissue with uniform cell distribution in 4 weeks.

After this period of static incubation, the silicone tubes with overlying cell sheets were mounted into the cyclic distension bioreactor and were stretched for 3 weeks (5% circumferential strain at 0.5 Hz), with or without axial constraints to tissue compaction. Tissue that was stretched, but not axially constrained, shortened extensively, leading to an

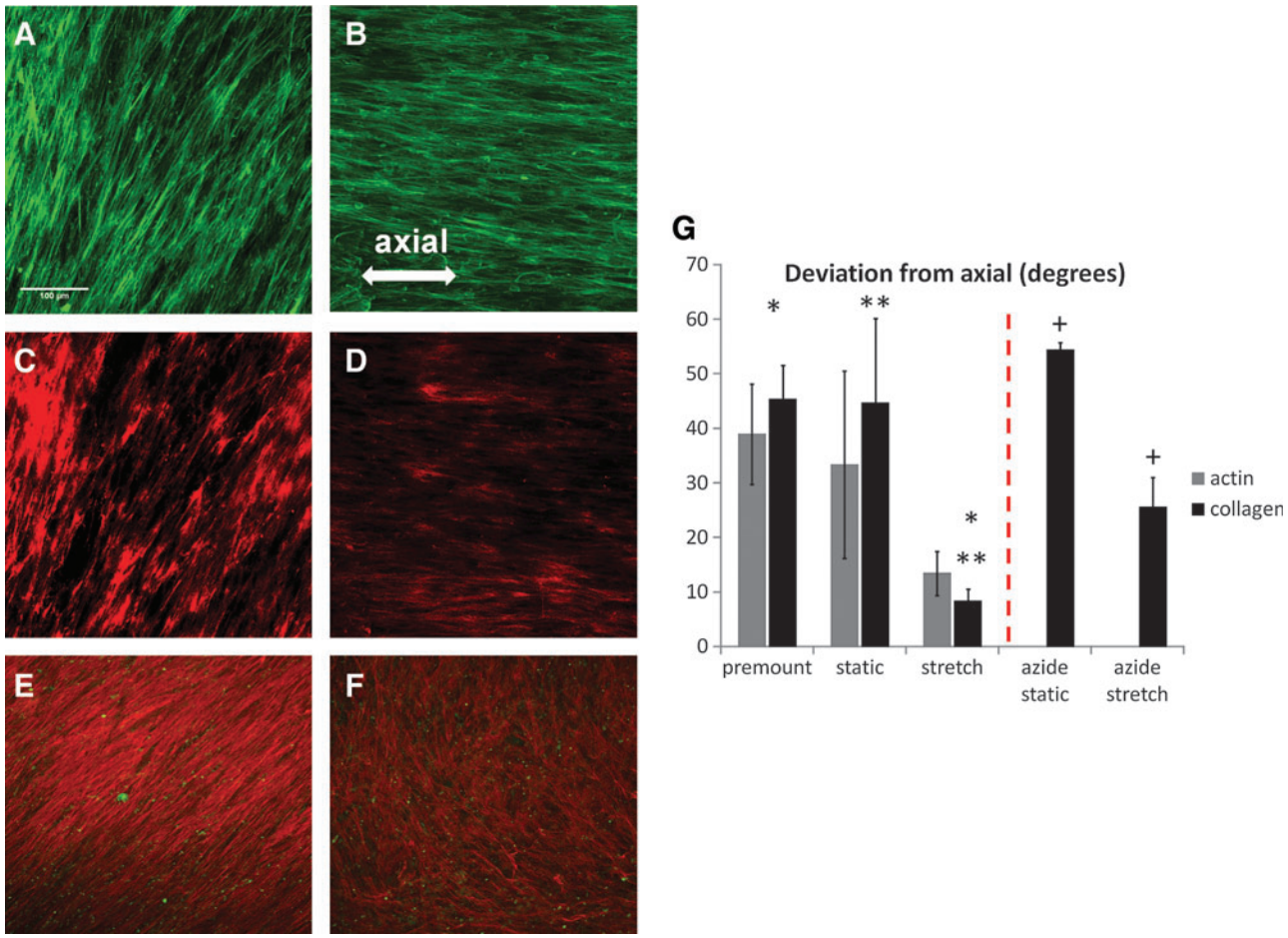

FIG. 7. Representative images of F-actin alignment in constrained tissue, **(A)** static and **(B)** stretched. Representative images of type I collagen alignment in **(C)** static and **(D)** stretched. Representative images of type I collagen alignment of azide-treated in **(E)** static and **(F)** stretched. **(G)** Quantification of tissue alignment with 2D fast Fourier transform. Paired symbols indicate a statistical difference ($p < 0.05$). Dashed line separates different experiments. Scale bar = 100 μm. Color images available online at www.liebertpub.com/tec

overall circumferential alignment of the tissue. The circumferential alignment of collagen did not improve intrinsic mechanical properties, consistent with a previous study of fibrin-based constructs with 5% cyclic stretch.[14] It is likely that the magnitude of stretch applied was not sufficient to increase collagen deposition and/or crosslinking in cell sheets. However, improvement in tensile properties with cyclic stretch can be achieved in tissue constructs with higher stretch magnitudes.[13,14,21–24] While the tissue compacted into a thicker structure, the collagen content as a percentage of total protein was slightly decreased due to mechanical stretching, which also may explain the lack of improvement in this study.

We also found that constraining the tissue axially to prevent shortening of the tissue during cyclic stretch prevented the development of circumferential alignment. To the contrary, the alignment of F-actin and collagen was found to be perpendicular to the stretch direction (i.e., axial). This suggests that without the ability to extensively compact the ECM axially (i.e., shorten the length of the tubular tissue), the cells aligned perpendicular to the stretch direction, a phenomenon known as strain avoidance. These results are similar to the response of fibroblasts on stretched membranes.[25,26]

When the influence of the cytoskeleton was removed by devitalizing the tissue with sodium azide, strong axial alignment of the collagen did not result with cyclic stretch. A similar result was recently reported by Foolen *et al.* when stretching collagen gel slabs containing entrapped cells. In this study, disruption of actin organization with a Rho associated protein kinase inhibitor diminished the strong alignment of collagen fibers seen in the untreated controls.[27] This suggests that, for the given experimental conditions, cytoskeletal tension influences collagen alignment. It also suggests the cells are directing the deposition and/or reorganization of collagen fibers, although it is not clear whether new collagen was being deposited in the direction of cell alignment or the cells were primarily reorganizing collagen existing prior to the stretching.

Several studies have shown that cells embedded in a matrix align with the direction of cyclic stretch. Gauvin *et al.* found that cell sheets maintained at 10% strain (static stretch) or cyclically stretched at 10% strain exhibited cell alignment in the stretch direction.[12] However, in this study the tissue compacted in the direction perpendicular to the stretching, making it difficult to determine if stretching or compaction led to cell alignment. Similarly, cyclic stretch induced alignment in the stretch direction has been reported by Seliktar *et al.* for cells entrapped in collagen gel subjected to 10% cyclic strain.[22,24] However, the collagen gel compacted perpendicular to the stretch direction during the experiment. Similar to a cell sheet, cell induced collagen gel compaction alone can directly cause alignment via a structural reorganization of the fiber network and subsequent cell alignment via contact guidance, so the true determinant of stretch induced alignment was confounded in these studies. In order to circumvent the confounding factor of compaction, Syedain *et al.* used fully compacted, circumferentially aligned fibrin-based tissue and subjected it to various circumferential stretching regimens. Increased circumferential alignment of collagen and cells was shown with 10% strain over a period of 5 weeks,[14] indicating that cells can align with the direction of cyclic stretching if they are prealigned via a contact guidance field existing in the tissue before stretching begins.

In our study, 5% circumferential cyclic stretch was insufficient to induce circumferential alignment of cells and collagen in a cell sheet, when the ends of the tissue were constrained. Instead, axial alignment of cells (based on F-actin) and collagen was observed. There are reports of cells at the surface of a 3D matrix aligning perpendicular to the stretch direction.[27–30] It is possible that because cell sheets are relatively thin, the cells behave more like cells at the surface of a thicker matrix, where the influence of contact guidance may be less pronounced.

Overall, this study indicates there is a coupling between internal, cell-generated tension associated with mechanical constraints on a tissue and external mechanical stretching, such that both factors need to be accounted for when determining the overall alignment of a tissue subjected to mechanical stretching. Future studies aim to determine the magnitude of mechanical stretching that is necessary to overcome the cell-generated tension, as well as how cell and collagen alignment vary as a function of tissue thickness.

Acknowledgments

The authors would like to acknowledge Naomi Ferguson, Sandy Johnson, Lee Meier, and Ben Hinton for technical assistance. Funding was provided by the NIH (HL083880) to R.T.T.

Disclosure Statement

No competing financial interests exist.

References

1. Lee, D.-Y., Yang, J.-M., and Park, K.-H. A dermal equivalent developed from fibroblast culture alone: effect of EGF and insulin. Wound Repair Regen **15,** 936, 2007.
2. L'heureux, N., Paquet, S., Labbe, R., Germain, L., and Auger, F.A. A completely biological tissue-engineered human blood vessel. FASEB J **12,** 47, 1998.
3. Takahashi, H., Nakayama, M., Shimizu, T., Yamato, M., and Okano, T. Anisotropic cell sheets for constructing three-dimensional tissue with well-organized cell orientation. Biomaterials **32,** 8830, 2011.
4. Isenberg, B.C., Backman, D.E., Kinahan, M.E., Jesudason, R., Suki, B., Stone, P.J., Davis, E.C., and Wong, J.Y. Micropatterned cell sheets with defined cell and extracellular matrix orientation exhibit anisotropic mechanical properties. J Biomech **45,** 756, 2012.
5. Williams, C., Xie, A.W., Emani, S., Yamato, M., Okano, T., Emani, S.M., and Wong, J.Y. A comparison of human smooth muscle and mesenchymal stem cells as potential cell sources for tissue-engineered vascular patches. Tissue Eng Part A **18,** 986, 2012.
6. See, E.Y.-S., Toh, S.L., and Goh, J.C.H. Multilineage potential of bone-marrow-derived mesenchymal stem cell cell sheets: implications for tissue engineering. Tissue Eng Part A **16,** 1421, 2011.
7. Kumashiro, Y., Yamato, M., and Okano, T. Cell attachment–detachment control on temperature-responsive thin surfaces for novel tissue engineering. Ann Biomed Eng **38,** 1977, 2010.
8. Yang, J., Yamato, M., Shimizu, T., Sekine, H., Ohashi, K., Kanzaki, M., Ohki, T., Nishida, K., and Okano, T. Re-

construction of functional tissues with cell sheet engineering. Biomaterials **28,** 5033, 2007.
9. Humphrey, J.D. Cardiovascular Solid Mechanics: Cells, Tissues, and Organs, 2nd ed. New York, NY: Springer-Verlag, 2002.
10. Pietak, A., McGregor, A., Gauthier, S., Oleschuk, R., and Waldman, S.D. Are micropatterned substrates for directed cell organization an effective method to create ordered 3D tissue constructs? J Tissue Eng Regen Med **2,** 450, 2008.
11. Grenier, G., Rémy-Zolghadri, M., Larouche, D., Gauvin, R., Baker, K., Bergeron, F., Dupuis, D., Langelier, E., Rancourt, D., Auger, F.A., and Germain, L. Tissue reorganization in response to mechanical load increases functionality. Tissue Eng **11,** 90, 2005.
12. Gauvin, R., Parenteau-Bareil, R., Larouche, D., Marcoux, H., Bisson, F., Bonnet, A., Auger, F.A., Bolduc, S., and Germain, L. Dynamic mechanical stimulations induce anisotropy and improve the tensile properties of engineered tissues produced without exogenous scaffolding. Acta Biomater **7,** 3294, 2011.
13. Isenberg, B.C., and Tranquillo, R.T. Long-term cyclic distention enhances the mechanical properties of collagen-based media-equivalents. Ann Biomed Eng **31,** 937, 2003.
14. Syedain, Z.H., Weinberg, J.S., and Tranquillo, R.T. Cyclic distension of fibrin-based tissue constructs: Evidence of adaptation during growth of engineered connective tissue. Proc Natl Acad Sci U S A **105,** 6537, 2008.
15. Tower, T.T., Neidert, M.R., and Tranquillo, R.T. Fiber alignment imaging during mechanical testing of soft tissues. Ann Biomed Eng **30,** 1221, 2002.
16. Stegemann, H., and Stalder, K. Determination of hydroxyproline. Clin Chim Acta **18,** 267, 1967.
17. Kim, Y.-J., Sah, R.L.Y., Doong, J.-Y.H., and Grodzinsky, A.J. Fluorometric assay of DNA in cartilage explants using Hoechst 33258. Anal Biochem **174,** 168, 1988.
18. Ayres, C.E., Jha, B.S., Meredith, H., Bowman, J.R., Bowlin, G.L., Henderson, S.C., and Simpson, D.G. Measuring fiber alignment in electrospun scaffolds: a user's guide to the 2D fast Fourier transform approach. J Biomater Sci Polym Ed **19,** 603,2008.
19. Nasseri, B.A., Pomerantseva, I., Kaazempur-Mofrad, M.R., Sutherland, F.W.H., Perry, T., Ochoa, E., Thompson, C.A., Mayer, J.E., Oesterle, S.N., and Vacanti, J.P. Dynamic rotational seeding and cell culture system for vascular tube formation. Tissue Eng **9,** 291, 2003.
20. Soletti, L., Nieponice, A., Guan, J., Stankus, J.J., Wagner, W.R., and Vorp, D.A. A seeding device for tissue engineered tubular structures. Biomaterials **27,** 4863, 2006.
21. Schutte, S.C., Chen, Z., Brockbank, K.G.M., and Nerem, R.M. Cyclic strain improves strength and function of a collagen-based tissue-engineered vascular media. Tissue Eng Part A **16,** 3149, 2010.
22. Seliktar, D., Nerem, R.M., and Galis, Z.S. Mechanical strain-stimulated remodeling of tissue-engineered blood vessel constructs. Tissue Eng **9,** 657, 2003.
23. Solan, A., Dahl, S.L.M., and Niklason, L.E. Effects of mechanical stretch on collagen and cross-linking in engineered blood vessels. Cell Transplant **18,** 915, 2009.
24. Seliktar, D., Black, R., Vito, R., and Nerem, R. Dynamic mechanical conditioning of collagen-gel blood vessel constructs induces remodeling *in vitro*. Ann Biomed Eng **28,** 351, 2000.
25. Boccafoschi, F., Bosetti, M., Gatti, S., and Cannas, M. Dynamic fibroblast cultures. Cell Adh Migr **1,** 124, 2007.
26. Kanda, K., and Matsuda, T. Behavior of arterial wall cells cultured on periodically stretched substrates. Cell Transplant **2,** 475, 1993.
27. Foolen, J., Deshpande, V.S., Kanters, F.M.W., and Baaijens, F.P. The influence of matrix integrity on stress-fiber remodeling in 3D. Biomaterials **33,** 7508, 2012.
28. Balestrini, J., Skorinko, J., Hera, A., Gaudette, G., and Billiar, K. Applying controlled non-uniform deformation for *in vitro* studies of cell mechanobiology. Biomech Model Mechanobiol **9,** 329, 2010.
29. Rubbens, M., Driessen-Mol, A., Boerboom, R., Koppert, M., van Assen, H., TerHaar Romeny, B., Baaijens, F., and Bouten, C. Quantification of the temporal evolution of collagen orientation in mechanically conditioned engineered cardiovascular tissues. Ann Biomed Eng **37,** 1263, 2009.
30. Boerboom, R.A., Rubbens, M.P., Driessen, N.J., Bouten, C.V., and Baaijens, F.P. Effect of strain magnitude of the tissue properties of engineered cardiovascular constructs. Ann Biomed Eng **36,** 244, 2008.

Address correspondence to:
Robert T. Tranquillo, PhD
Department of Biomedical Engineering
University of Minnesota
7-114 NHH
312 Church St. SE
Minneapolis, MN 55455

E-mail: tranquillo@umn.edu

Received: July 11, 2012
Accepted: October 15, 2012
Online Publication Date: January 8, 2013

(Appendix follows →)

Appendix

Experimental Group	Number of Samples (N)
Cell Seeding, 0.4M/ml	N=5
Cell Seeding, 1.0 M/ml	N=5
Cell Seeding, 2.0 M/ml	N=4
Cell Seeding, 4 hours	N=6
Cell Seeding, Overnight	N=6
Unconstrained, Static - Mechanics	N=3
Unconstrained, Stretch – Mechanics	N=4
Unconstrained, Static – Dimensions	N=5
Unconstrained, Stretch – Dimensions	N=5
Unconstrained, Static – Biochemistry	N=3
Unconstrained, Stretch – Biochemistry	N=3
Constrained, Premount - Collagen	N=4
Constrained, Static - Collagen	N=5
Constrained, Stretch - Collagen	N=4
Constrained, Premount - f-actin	N=3
Constrained, Static - f-actin	N=5
Constrained, Stretch - f-actin	N=5
Constained, Azide + Static - Collagen	N=2
Constrained, Azide + Stretch - Collagen	N=2

APPENDIX FIG. A1. Table of number of samples (N) per experimental group.